

## MAGNETIC FIELD EFFECT ON CONVECTIVE HEAT TRANSFER IN CORRUGATED FLOW CHANNEL

by

**Hadi HEIDARY<sup>a</sup>, Mohammad Jafar KERMANI<sup>a\*</sup>, and Bahram DABIR<sup>b</sup>**

<sup>a</sup>Department of Mechanical Engineering, Amirkabir University of Technology  
Tehran, Iran

<sup>b</sup>Department of Chemical Engineering, Amirkabir University of Technology  
Tehran, Iran

Original scientific paper  
<https://doi.org/10.2298/TSCI140610002H>

*In this study heat transfer and fluid flow analysis in a wavy channel is numerically studied, while a magnetic field is applied in transverse direction to the main flow stream. Recently in a numerical study, we have observed that usage of wavy channel instead of straight one enhances heat exchange between the core flow and hot walls. On the other hand, the usage of magnetic field transverse to hot walls can enhance heat transfer in a straight channel. In this paper, we would like to examine if presence of these two methods simultaneously is useful for enhancement of heat exchange. For this purpose, the governing equations are numerically solved in the domain by the control volume approach based on the SIMPLE technique. Numerical studies are performed over a range of Reynolds number, Hartmann number, and the wave amplitude. From this study, it is concluded that heat transfer in channels can be enhanced by the usage of magnetic field or usage of wavy channel instead of a straight one. But simultaneous usage of magnetic field and wavy channel is not recommended.*

Key words: forced convection, magnetic field, MHD, wavy, channel

### Introduction

Forced convection in a channel is one of the most important subjects in many technological applications like heat exchangers, high performance boilers, chemical catalytic reactors, solar collectors, power plants, thermal desalination systems, and cooling systems. Management of heat transfer for its enhancement or reduction in these systems is an essential task from an energy saving perspective.

One useful method for enhancement of convective heat transfer is the usage of wavy or indenting channel instead of the straight one. The wavy wall channel is one of several devices employed for enhancing the heat transfer efficiency of industrial transport processes. Wang and Chen [1] analyzed forced convection heat transfer through a sinusoidal channel using a simple co-ordinate transformation method and the spline alternating direction implicit method. Their results showed that the amplitudes of the Nusselt number and the skin friction coefficient increase with an increase in the Reynolds number and the amplitude wave length ratio. Jafari *et al.* [2] have investigated effects of the pulsating flow on forced convection in a corrugated channel using lattice Boltzmann method based on boundary fitting method. Ferley and Ormiston [3]

\*Corresponding author, e-mail: mkermani@aut.ac.ir

have computed laminar forced convection in channels with different geometries and showed that rounded-ellipse-shaped corrugation has the highest heat transfer per unit pumping power at an inlet Reynolds number of 300. Taymaz and Parmaksizoglu [4] experimentally determined forced convection heat transfer coefficients and friction factor for air-flowing in corrugated channel. They showed that with channel height of 5 mm, Nusselt number exceeds the straight value by 15% at  $Re = 1200$  and about 75% at  $Re = 4000$ .

Naphon [5] experimentally presented the results of the heat transfer characteristics and pressure drop in the corrugated channel under constant heat flux. The test section was the channel with two opposite corrugated plates which all configuration peaks lie in an in-line arrangement. This study showed that Nusselt number increases with increasing wavy angle. Ahmed *et al.* [6, 7] have investigated heat transfer and pressure drop characteristics of Cu-water nanofluid flow through isothermally heated corrugated and wavy channel in two separate studies. They also showed that increase in wave amplitude from 0.1 to 0.3, can enhance heat transfer by a factor of 1.5 in case of pure fluid in  $Re = 500$ . Heidary and Kermani [8] computed the forced convection heat transfer enhancement and hydrodynamics of the flow field in a wavy channel with nanofluids. They concluded that the heat transfer can be enhanced up to 50%. In another study Heidary and Kermani [9] repeated similar problem in channel with partial blocks installed in bottom wall of the channel. Yang and Chen [10], Taymaz and Islamoglu [11], Zimparov and Penchev [12], Heidary and Kermani [13], and Wu and Zhou [14] have also reported similar investigations on the effect of corrugated channels with different corrugation shapes on enhancement of forced convection heat transfer.

The other way for enhancement of convective heat transfer is the usage of magnetic field. The study of an electrically conducting fluid in engineering applications is of considerable interest, especially in metallurgical and metal working processes or in separation of molten metals from non-metallic inclusions by the application of a magnetic field. In that case the fluid experiences a Lorentz force. This in turn affects the rate of heat and mass transfer.

Natural convection flow in the presence of a magnetic field in enclosure heated from one side and cooled from the other side was considered by Ece and Buyuk [15] and Jue [16]. Mahmoudi *et al.* [17] have studied natural convection for a 2-D triangular enclosure with partially heated from below and cold inclined wall filled with nanofluid in presence of magnetic field. Ghasemi *et al.* [18] examined the natural convection in an enclosure that is filled with a  $Al_2O_3$ -water nanofluid and in the influence of a magnetic field. Davoudian and Arab Solghar [19] examined buoyancy-driven fluid flow and heat transfer in a square cavity containing nanofluid with a vertical plate at the center under magnetic field. Jena *et al.* [20] studied thermogravitational convection of an electrically conducting fluid in a rectangular annular space under the influence of an externally imposed time independent uniform magnetic field. Nemati *et al.* [21] applied the lattice Boltzmann method to investigate the effect of CuO nanoparticles on natural convection with MHD flow in a square cavity. Aminossadati *et al.* [22] examined the laminar forced convection of a  $Al_2O_3$ -water nanofluid flowing through a horizontal micro-channel. They have shown the presence of nanoparticles and usage of magnetic field transverse to hot walls can enhance heat transfer in a straight channel up to 75%.

As mentioned previously, both magnetic field and corrugated (wavy) channels are useful ways to enhance forced convective heat transfer between the hot wall and core flow. In this paper, the effect of magnetic field and wavy wall are both individually and simultaneously investigated. The main aim of this paper is that we would like to show whether simultaneous presence of these two techniques are useful for enhancement of the heat exchange between hot walls and core flow or not.

To the best of our knowledge no comprehensive model has been published so far in the literature to study convective heat transfer in a wavy channel with magnetic field transverse to flow field for enhancement of heat exchange between fluid and hot wall. The fluid temperature at the channel inlet,  $T_C$ , is taken less than that of the walls,  $T_W$ . The effects of the Reynolds number, Hartmann number, and the wave amplitude on Nusselt number and friction factor are also investigated in the present study.

**Governing equations**

Consider a 2-D channel as shown in fig. 1 with the opening height  $2H$  and length  $L$ . The computations were carried out with the assumption of a 2-D model same as Aminossadati et al. [22]. Magnetic field is applied in y-direction. The temperature of the horizontal walls  $T_W$  are taken such that  $T_W > T_C$ , where  $T_C$  is the fluid temperature at the inlet plane. The governing equations in both dimensional and non-dimensional forms are given:

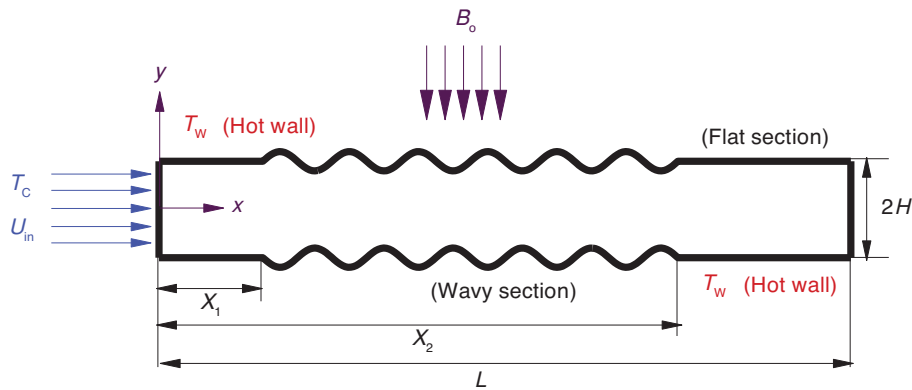


Figure 1. Schematic diagram of the duct studied here

*Dimensional form of the governing equations*

The continuity, momentum, and energy equations can be expressed:

$$\frac{\partial u}{\partial x} + \frac{\partial v}{\partial y} = 0 \tag{1}$$

$$u \frac{\partial u}{\partial x} + v \frac{\partial u}{\partial y} = -\frac{1}{\rho} \frac{\partial p}{\partial x} + \frac{\mu}{\rho} \left( \frac{\partial^2 u}{\partial x^2} + \frac{\partial^2 u}{\partial y^2} \right) - \frac{\sigma B_0^2}{\rho} u \tag{2}$$

$$u \frac{\partial v}{\partial x} + v \frac{\partial v}{\partial y} = -\frac{1}{\rho} \frac{\partial p}{\partial y} + \frac{\mu}{\rho} \left( \frac{\partial^2 v}{\partial x^2} + \frac{\partial^2 v}{\partial y^2} \right) \tag{3}$$

$$u \frac{\partial T}{\partial x} + v \frac{\partial T}{\partial y} = \frac{k}{\rho c_p} \left( \frac{\partial^2 T}{\partial x^2} + \frac{\partial^2 T}{\partial y^2} \right) \tag{4}$$

where  $u$  and  $v$  are the velocity components along  $x$ - and  $y$ -axes,  $p$  is the pressure,  $T$  – the fluid temperature,  $B_0$  – the magnitude of magnetic field, and  $\sigma$  – the electrical conductivity.

The boundary conditions for the previous dimensional system are defined according to the geometry of fig. 1:

$$\begin{aligned}
\text{– exit plane} & \quad \frac{\partial T}{\partial x} = 0, \quad \frac{\partial u}{\partial x} = 0 \quad \text{at } x = L \text{ and } -H \leq y \leq H \\
\text{– top wall} & \quad T = T_w, \quad u = v = 0 \quad \text{at } y = H \\
\text{– bottom wall} & \quad T = T_w, \quad u = v = 0 \quad \text{at } y = -H \\
\text{– inflow} & \quad T = T_c, \quad u = U_{in}, \quad v = 0 \quad \text{at } x = 0 \text{ and } -H \leq y \leq H
\end{aligned} \tag{5}$$

#### Non-dimensional form of the governing equations

The continuity, momentum, and energy equations are expressed in the non-dimensional form in this section using the following dimensionless parameters:

$$\begin{aligned}
X = \frac{x}{H}, \quad Y = \frac{y}{H}, \quad U = \frac{u}{U_{in}}, \quad V = \frac{v}{U_{in}}, \quad P = \frac{p}{\rho U_{in}^2}, \quad \theta = \frac{T - T_c}{T_w - T_c}, \\
\text{Re}_H = \frac{\rho U_{in} H}{\mu}, \quad \text{Pr} = \frac{\mu c_p}{k}
\end{aligned} \tag{6}$$

Then the non-dimensional equations will be:

$$\frac{\partial U}{\partial X} + \frac{\partial V}{\partial Y} = 0 \tag{7}$$

$$U \frac{\partial U}{\partial X} + V \frac{\partial U}{\partial Y} = -\frac{\partial P}{\partial X} + \frac{1}{\text{Re}} \left( \frac{\partial^2 U}{\partial X^2} + \frac{\partial^2 U}{\partial Y^2} \right) - \frac{\text{Ha}^2}{\text{Re}} U \tag{8}$$

$$U \frac{\partial V}{\partial X} + V \frac{\partial V}{\partial Y} = -\frac{\partial P}{\partial Y} + \frac{1}{\text{Re}} \left( \frac{\partial^2 V}{\partial X^2} + \frac{\partial^2 V}{\partial Y^2} \right) \tag{9}$$

$$U \frac{\partial \theta}{\partial X} + V \frac{\partial \theta}{\partial Y} = \frac{1}{\text{Pr Re}} \left( \frac{\partial^2 \theta}{\partial X^2} + \frac{\partial^2 \theta}{\partial Y^2} \right) \tag{10}$$

The effect of the electromagnetic field is introduced into the equations of motion (8) through Hartmann number and it is defined:

$$\text{Ha} = B_0 H \sqrt{\frac{\sigma}{\rho \nu}} \tag{11}$$

The corresponding boundary conditions in the non-dimensional system are:

$$\begin{aligned}
\text{– exit plane} & \quad \frac{\partial \theta}{\partial X} = 0, \quad \frac{\partial U}{\partial X} = 0 \quad \text{at } X = \frac{L}{H} \text{ and } -1 \leq Y \leq 1 \\
\text{– top wall} & \quad \theta = 1, \quad U = V = 0 \quad \text{at } Y = 1 \\
\text{– bottom wall} & \quad \theta = 1, \quad U = V = 0 \quad \text{at } Y = -1 \\
\text{– inflow} & \quad \theta = 0, \quad U = 1, \quad V = 0 \quad \text{at } X = 0 \text{ and } -1 \leq Y \leq 1
\end{aligned} \tag{12}$$

The local variation of the Nusselt number along the top and bottom hot walls is defined:

$$\text{Nu} = -\frac{\frac{\partial T}{\partial n} H}{T_w - T_c} \quad (13)$$

where

$$\frac{\partial T}{\partial n} = \bar{\nabla} T \hat{n} = \left( \frac{\partial T}{\partial x} \hat{i} + \frac{\partial T}{\partial y} \hat{j} \right) (\cos \xi \hat{i} + \sin \xi \hat{j}) \quad (14)$$

where  $\xi$  is the slope of the wall. The average Nusselt number is calculated by integrating the local Nusselt number over the walls. Hot wall average Nusselt number:

$$\bar{\text{Nu}} = \frac{1}{S} \int_0^S \text{Nu} \, ds \quad (15)$$

where  $s$  and  $S$  are hot wall geometry and the total length of the horizontal walls. The shear stress and skin friction coefficient at the wall are calculated from:

$$\tau_w = \mu \left( \frac{\partial u}{\partial y} + \frac{\partial v}{\partial x} \right)_{y=s(x)} \quad (16)$$

$$C_f = \frac{\tau_w}{\rho U_{in}^2} \quad (17)$$

### Numerical method

The present computation uses the finite volume method and the SIMPLE algorithm [23] to discretize the governing equations of flow and resolving the pressure-velocity coupling system. In addition, all the variables are stored in same nodes by using collocated grid. This method was suggested by Rhie and Chow [24]. Collocated grid has various advantages over the staggered grid, *e. g.* the control volumes for all variables coincide with the boundaries of the solution domain, to facilitate the enforcement of boundary conditions, and giving a simplified data storage structure.

In present CFD code, three different discretization schemes are available to approximate the convective terms: upwind/central difference and hybrid schemes. In this study, the convection and diffusion terms of the equations are discretized by central difference scheme. The strongly implicit procedure algorithm is used to solve the obtained algebraic equations. The convergence criterion,  $10^{-5}$  is chosen for all dependent variables, where the computation is terminated if:

$$\frac{\sum_{i,j} |A_{i,j}^n - A_{i,j}^{n-1}|}{\sum_{i,j} |A_{i,j}^n|} \leq 10^{-5}$$

Here  $A$  stands for either temperature or velocity components, and  $n$  denotes the iteration step. Further details about the numerical method are given in Ferziger and Peric [25].

For the wavy channel a non-orthogonal grid was used for grid generation. The grid independency test was performed with four grid levels  $40 \times 100$ ,  $70 \times 200$ ,  $100 \times 300$ , and  $120 \times 400$ . In all cases a unified grid clustering factor near to the wall has been used. It is observed that grids  $70 \times 200$ , can adequately resolve the physics of the problem and further refinement is unnecessary. This grid and an enlarged view of the wavy wall are shown in fig. 2.

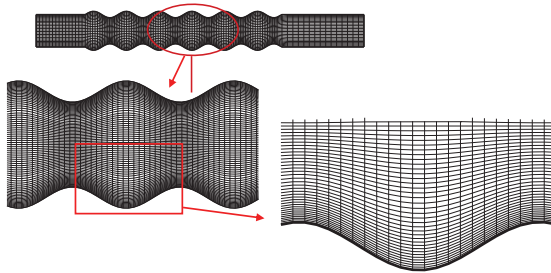


Figure 2. A sample of grid configuration used in the present computation

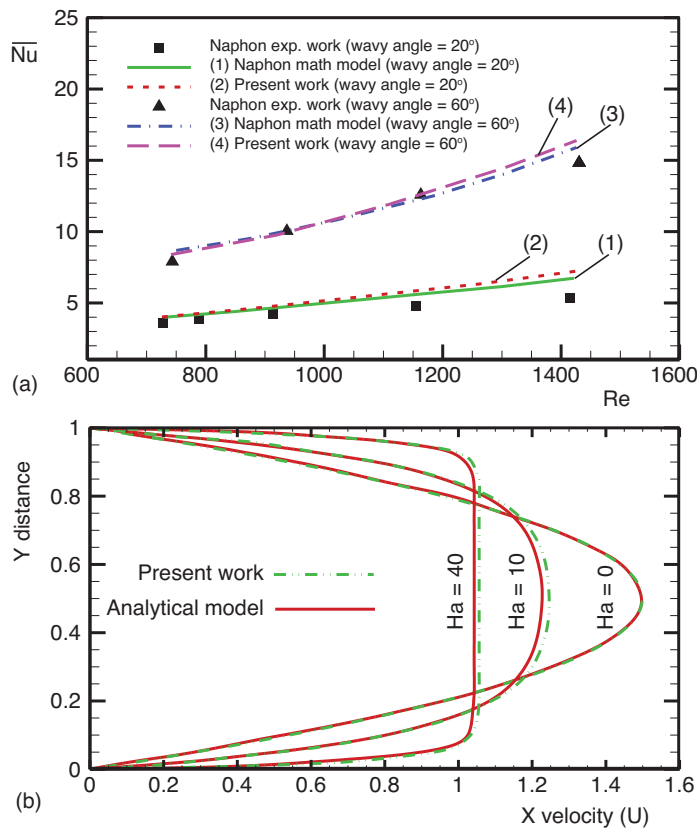


Figure 3. (a) Validation of the present code with experimental and numerical results obtained from [5] for corrugated channel in different Reynolds numbers, (b) Validation of the present code with analytical solution [26] for two parallel plates flow under magnetic field

behavior near the channel walls. As shown in this figure, the thermal boundary layer thins with presence of magnetic field, *i. e.*  $\delta_{t,MHD} \delta_{t,f} < 1$ , where  $\delta_{t,f}$  and  $\delta_{t,MHD}$  are, respectively, the thermal boundary layer thicknesses without and with magnetic field.

## Results and discussion

### Validations

In order to assess the accuracy of our numerical procedure, we have tested our algorithm *vs.* several test cases. The first test case studied is the comparison of results obtained from present code for forced convection in corrugated channel with experimental and numerical results of Naphon [5]. As can be seen from fig. 3(a), good agreement with the data obtained from the literature has been obtained.

The present CFD code is also validated with results of a MHD flow obtained from an analytical model developed by Back [26]. The results of the fully developed velocity profile are presented for three different Hartmann numbers in fig. 3(b). This figure shows a very good agreement between the present study and literature.

### Results

The present computations have been carried out for  $Re = 10$  to  $1000$ ,  $Pr = 7.02$ ,  $Ha = 0$  to  $60$ , and dimensionless wave amplitudes,  $\alpha = 0$  to  $0.3$  ( $\alpha = a/H$ ; where  $a$  is dimensional wave amplitude). The results of the computations are shown in figs. 4-8.

Figure 4 shows non-dimensional isotherm lines,  $\theta$ , for the cases of without magnetic field ( $Ha = 0$ ) and with magnetic field ( $Ha = 30$ ) in  $Re = 25$  and  $250$  to compare the effect of Hartmann number in wavy-corrugated channel with  $\alpha = 0.2$ . The enlarged figures show clearly the isotherm lines be-

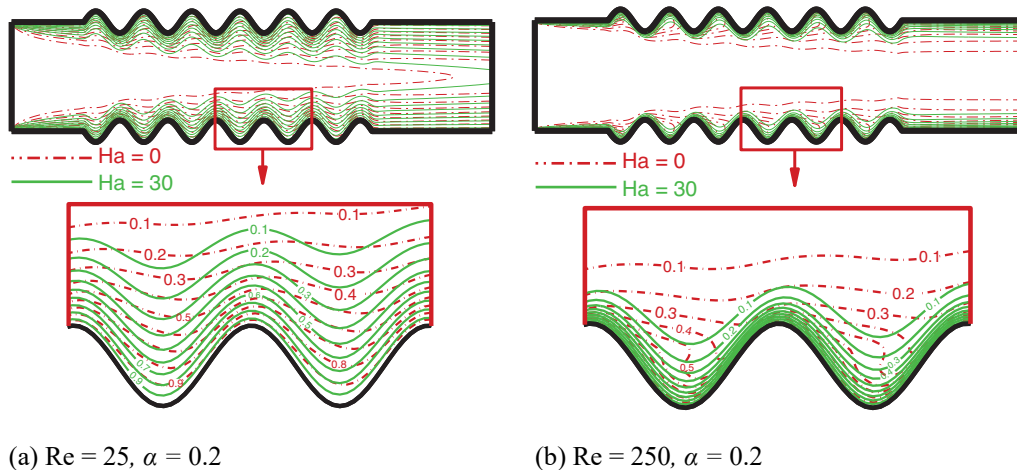


**Figure 4. Comparisons of dimensionless isotherm contours ( $\theta$ ) obtained in the present study with  $Ha = 0$  and  $30$  in (a)  $Re = 25$  and (b)  $Re = 250$**

This shows that with magnetic field, the velocity gradient near the wall increases intensely. Because with magnetic field, the Lorentz force is generated at the middle section of the channel. This force decreases the velocity at the center side of the channel, please see negative term in right hand side of momentum equation, eq. (8). So with assuming constant mass flow along the duct, flow velocity increases greatly near the hot walls and this, in turn, enhances temperature gradient and heat exchange between horizontal walls and core flow (of course in flat section and corrugation troughs, not in crest/bump; the reason will be mentioned later).

Figures 4(a) and 4(b) also shows the effect of Reynolds number on isotherms. As the flow Reynolds number increases, the boundary layer shrink, hence the isotherm lines gravitate toward the walls. This increases the temperature gradient near the wall. So the Nusselt number and the heat exchange enhance.

In terms of the hydrodynamics, streamline contours along the wavy channel with  $\alpha = 0.2$  for various Hartmann number are depicted in figs. 5(a)-5(e). As shown in figs. 5(a) and 5(b), with increasing of the cross-sectional area in each wave, a vortex is formed within the cavity portion of the wave (corrugation trough). In other words, corrugated boundary increases fluid re-circulation which is generated in the corrugation troughs and therefore, the mixing of fluid increases in the boundary layer. This in turn enhances convective heat transfer and local Nusselt number near the bumps (crest) of corrugated wall. With applying magnetic field, flow velocity increases greatly near the hot walls and vortex strength decreases with Hartmann number, please see figs. 5(c)-5(e). In case of  $Ha = 20$ , the vortex are totally vanished.

Figures 6(a) and 6(b) show variation of local Nusselt number along the duct for different values of wave amplitudes  $\alpha$  and Hartmann numbers. Figure 6(a) shows the profiles of the local Nusselt number along the wavy channel at various wave amplitudes  $\alpha = 0, 0.1, 0.2,$  and  $0.3$  without magnetic field ( $Ha = 0$ ). As shown in this figure, when  $\alpha$  increases the throat openings become narrower. Hence fluid re-circulation will be raised in the corrugation troughs and the mixing of fluid increases in the boundary layer. Then the local Nusselt number enhances. It should be noted that although in re-circulation zone, local Nusselt number is very low, but presence of this re-circulation leads to flow mixing in boundary layer and heat transfer enhancement.

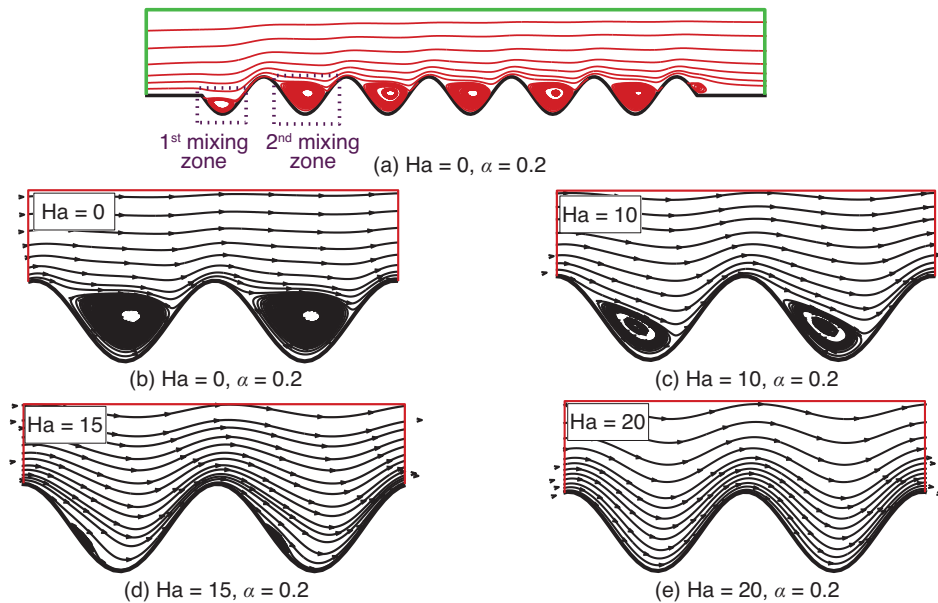


**Figure 5.** Comparisons of streamline contours of wavy-corrugated channel ( $\alpha = 0.2$ ) obtained in the present study for different Hartmann numbers at  $Re = 250$

Figure 6(b) shows the profiles of the local Nusselt number along the wavy channel at various Hartmann numbers,  $Ha = 0, 10, 30,$  and  $60$ . As shown in this figure, when Hartmann number increase, flow velocity increases greatly near the hot walls and this enhances temperature gradient and heat exchange between horizontal walls and core flow in flat section and corrugation troughs of the wall, see fig. 6(b). But heat exchange decreases near the crests with Hartmann number. The reason is as follows.

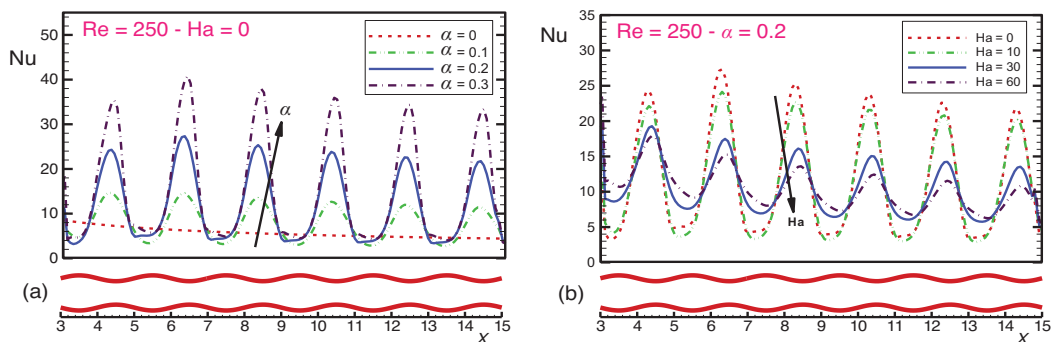


**Figure 6.** Sample of parametric studies in the present computation; (a) effect of wave amplitude on distribution of local Nusselt number, (b) effect of Hartmann number on distribution of local Nusselt number

Although boundary layer thickness decreases with magnetic field as shown in fig. 4, but magnetic field also decreases fluid re-circulation which is generated in the corrugation troughs and therefore, the mixing of fluid decreases in the boundary layer and the enhancement of convective heat transfer near the crest is damped with Hartmann number. Therefore the peak value of the local Nusselt number decreases with Hartmann number. From two these figures

we can conclude although waviness of channel walls improves heat exchange between core flow and channel surfaces, but magnetic field to neutralize the corrugation effect.

Figure 7 shows the variation of average Nusselt number of the hot walls of channels vs. Hartmann numbers for different wave amplitude (0, 0.1, 0.2, and 0.3). As shown in this figure, as Hartmann number increases, the  $\overline{Nu}$  increases in straight channel. The reason is explained as follows: with magnetic field, the Lorentz force is generated at the middle section of the channel and the flow velocity at the center side of the channel decreases. So with assuming constant mass flow along the duct, flow velocity increases greatly near the hot walls and this, in turn, enhances temperature gradient and heat exchange between horizontal walls and core flow. Also noted in this figure, in a specified Hartmann number, as the amplitude of the wavy walls,  $\alpha$ , increases, the  $\overline{Nu}$  increases too. This is due to the increased disturbance sizes introduced to the main flow at increased  $\alpha$  values.

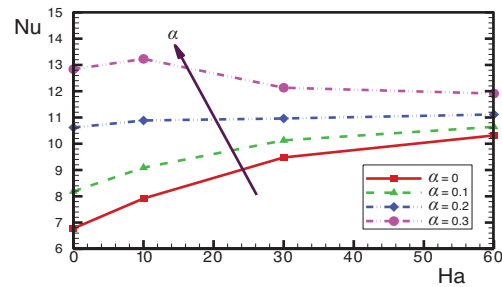


Figure 7. Sample of parametric studies in the present computation; diagram of Nusselt vs. Hartmann numbers for various wave amplitude at  $Re = 250$

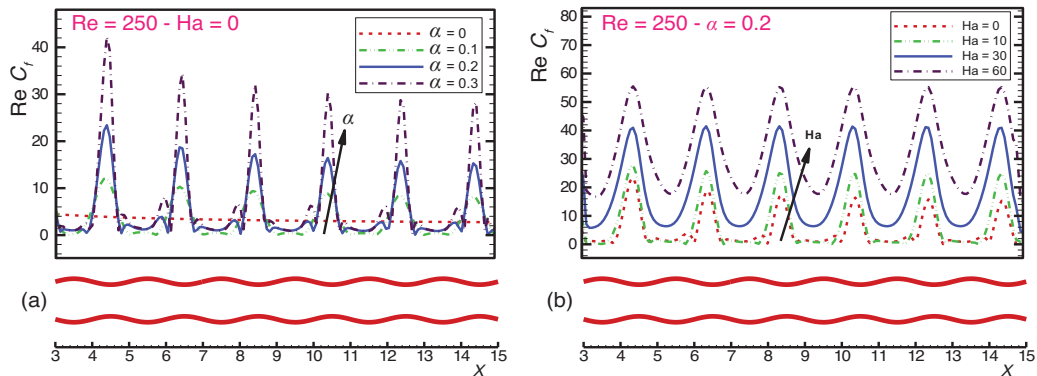


Figure 8. Sample of parametric studies in the present computation; (a) effect of wave amplitude on distribution of friction factor ( $Re C_f$ ), (b) effect of Hartmann number on distribution of friction factor ( $Re C_f$ )

The very important point in this figure is that in high wave amplitude ( $\alpha \geq 0.2$ ), magnetic field has slight effect on heat transfer enhancement. Because with magnetic field in corrugated channel, although heat exchange in flat section and corrugation troughs (mixing zone) of channel enhances, the local Nusselt number bumps are damped due to reducing of fluid mixing with Hartmann number. For example, in straight channel ( $\alpha = 0$ ) applying magnetic field with  $Ha = 60$ , increases heat exchange by a factor 1.5, but in wavy wall channel with  $\alpha = 0.2$ , magnetic field with  $Ha = 60$ , increases heat exchange to less than 5%. Even in  $\alpha = 0.3$ , presence of magnetic field has an adverse effect and decreases the heat exchange. Also, observed in this figure, with the absence of magnetic field, the construction of wavy hot wall with wave amplitude  $\alpha = 0.2$  instead of straight one, enhance heat exchange between the core flow and hot walls by a factor 1.55, but with presence of magnetic field with  $Ha = 60$ , the construction of wavy wall with wave amplitude  $\alpha = 0.2$ , has slight change on heat exchange enhancement (less than about 8%). Indeed, this figure shows that presence of magnetic field and wavy wall

simultaneously is not useful for heat transfer enhancement, whereas any one of these methods are useful ways for heat exchange enhancement individually.

Variations of the skin friction coefficient,  $C_f$ , along the duct are shown in figs. 8(a) and 8(b). These profiles are depicted at various  $\alpha$  and Hartmann number values. As shown in these figures, when the duct cross-sectional area reduces (at the duct throats) a jump in the  $C_f$  profiles is observed. This is because the velocity gradient at the wall increases in throat regions. The effect of wave amplitude  $\alpha$  on the  $C_f$  is depicted in fig. 8(a). With  $\alpha$ , although both Nusselt number and heat exchange enhance, but this enhancement is accompanied with increase in  $C_f$  and pressure drop. The effect of magnetic field Hartmann number on the  $C_f$  is depicted in fig. 8(b). With Hartmann number, also velocity gradient increases near the wall and this, in turn, increases  $C_f$  and pressure drop along the duct.

## Conclusions

A parametric study on the effect of magnetic strength (Hartmann number) on the enhancement of heat exchange between an isothermal duct with wavy wall and the core flow has been presented in this paper.

The most important result of this study is that presence of magnetic field and wavy wall simultaneously is not suitable for heat transfer enhancement, whereas any one of these methods would be useful for heat exchange enhancement individually. For example, in straight channel ( $\alpha = 0$ ) the presence of magnetic field with strength of  $Ha = 60$ , increase heat exchange by a factor of 1.5, but in wavy wall channel with  $\alpha = 0.2$ , magnetic field with  $Ha = 60$ , increase heat exchange is less than 5%.

## Nomenclature

$a$	– dimensional wave amplitude, [m]	$X, Y$	– dimensionless horizontal and vertical co-ordinates
$B_o$	– magnetic field, [ $Wb\ m^{-2}$ ]	$X_1, X_2$	– start point and end point of wavy section, [m]
$C_f$	– skin friction coefficient, [-]	$x, y$	– horizontal and vertical co-ordinates, [m]
$c_p$	– specific heat of fluid, [ $J\ kg^{-1}\ K^{-1}$ ]	<i>Greek symbols</i>	
$H$	– half the opening height of the channel, [m]	$\alpha$	– dimensionless wave amplitude [ $aH^{-1}$ ]
$Ha$	– Hartmann number	$\delta$	– boundary layer thickness, [m]
$k$	– thermal conductivity, [ $W\ m^{-1}\ K^{-1}$ ]	$\zeta$	– the angle between horizontal and wavy wall
$L$	– length of the channel, [m]	$\theta$	– dimensionless temperature
$Nu$	– local Nusselt number	$\mu$	– dynamic viscosity, [ $N\ s\ m^{-2}$ ]
$\bar{Nu}$	– average Nusselt number	$\nu$	– kinematic viscosity, [ $m^2\ s^{-1}$ ]
$P$	– dimensionless pressure	$\rho$	– density, [ $kg\ m^{-3}$ ]
$Pr$	– Prandtl number, [ $\mu c_p\ k^{-1}$ ]	$\sigma$	– electrical conductivity, [ $\mu S\ cm^{-1}$ ]
$p$	– pressure, [ $N\ m^{-2}$ ]	$\tau$	– shear stress, [ $N\ m^{-2}$ ]
$Re$	– Reynolds number	<i>Subscripts</i>	
$S$	– total wall length of the hot wall, [m]	C	– cold wall
$s$	– hot wall geometry, [m]	in	– input boundary
$T$	– temperature, [K]	W	– hot wall
$T_w, T_c$	– temperature of the hot and cold wall, [K]		
$U, V$	– dimensionless velocity components		
$u, v$	– velocity components, [ $ms^{-1}$ ]		

## Reference

- [1] Wang, C. C., Chen, C. K., Forced Convection in a Wavy-Wall Channel, *International Journal of Heat and Mass Transfer*, 45 (2002), 12, pp. 2587-595
- [2] Jafari, M., et al., Pulsating Flow Effects on Convection Heat Transfer in a Corrugated Channel: A LBM Approach, *International Communications in Heat and Mass Transfer*, 45 (2013), July, pp. 146-154

- [3] Ferley, D. M., Ormiston, S. J., Numerical Analysis of Laminar Forced Convection in Corrugated-Plate Channels with Sinusoidal, Ellipse, and Rounded-vee Wall Shapes, *Numerical Heat Transfer, Part A: Applications*, 63 (2013), 8, pp. 563-589
- [4] Taymaz, Y., Parmaksizoglu, C., The Effect of Channel Height on the Enhanced Heat Transfer Characteristics in a Corrugated Heat Exchanger Channel, *Applied Thermal Engineering*, 23 (2003), 8, pp. 979-987
- [5] Naphon, P., Effect of Corrugated Plates in an In-Phase Arrangement on the Heat Transfer and Flow Developments, *International Journal of Heat and Mass Transfer*, 51 (2008), 15-16, pp. 3963-3971
- [6] Ahmed, M. A., et al., Numerical Investigations on the Heat Transfer Enhancement in a Wavy Channel Using Nanofluid, *International Journal of Heat and Mass Transfer*, 55 (2012), 21-22, pp. 5891-5898
- [7] Ahmed, M. A., et al., Numerical Investigations of Flow and Heat Transfer Enhancement in a Corrugated Channel Using Nanofluid, *International Communications in Heat and Mass Transfer*, 38 (2011), 10, pp. 1368-1375
- [8] Heidary, H., Kermani, M. J., Effect of Nano-Particles on Forced Convection in Sinusoidal-Wall Channel, *International Communications in Heat and Mass Transfer*, 37 (2010), 10, pp. 1520-1527
- [9] Heidary, H., Kermani, M. J., Heat Transfer Enhancement in a Channel with Block (S) Effect and Utilizing Nano-Fluid, *International Journal of Thermal Sciences*, 57 (2012), July, pp. 163-171
- [10] Yang, Y. T., Chen, P. J., Numerical Simulation of Fluid Flow and Heat Transfer Characteristics in Channel with V Corrugated Plates, *Heat and Mass Transfer*, 46 (2010), 4, pp. 437-445
- [11] Taymaz, I., Islamoglu, Y., Prediction of Convection Heat Transfer in Converging-Diverging Tube for Laminar Air Flowing Using Back-Propagation Neural Network, *International Communications in Heat and Mass Transfer*, 36 (2009), 6, pp. 614-617
- [12] Zimparov, V., Penchev, P. J., Performance Evaluation of Deep Spirally Corrugated Tubes for Shell-and-Tube Heat Exchangers, *Journal of Enhanced Heat Transfer*, 11 (2004), 4, pp. 423-434
- [13] Heidary, H., Kermani, M. J., Performance Enhancement of Fuel Cells Using Bipolar Plate Duct Indentations, *International Journal of Hydrogen Energy*, 38 (2013), 13, pp. 5485-5496
- [14] Wu, F., Zhou, W., Numerical Simulation and Optimization of Convective Heat Transfer and Pressure Drop in Corrugated Tubes, *Heat Transfer Research*, 43 (2012), 6, pp. 527-544
- [15] Ece, M. C., Buyuk, E., Natural Convection Flow under a Magnetic Field in an Inclined Rectangular Enclosure Heated and Cooled on Adjacent Walls, *Fluid Dynamics Research*, 38 (2006), 8, pp. 564-590
- [16] Jue, T., Analysis of Combined Thermal and Magnetic Convection Ferrofluid Flow in a Cavity, *International Communications in Heat and Mass Transfer*, 33 (2006), 7, pp. 846-852
- [17] Mahmoudi, A. H., et al., Effect of Magnetic Field on Natural Convection in a Triangular Enclosure Filled with Nanofluid, *International Journal of Thermal Sciences*, 59 (2012), Sept., pp. 126-140
- [18] Ghasemi, B., et al., Magnetic Field Effect on Natural Convection in a Nanofluid Field Square Enclosure, *International Journal of Thermal Sciences*, 50 (2011), 9, pp. 1748-1756
- [19] Davoudian, M., Arab Solghar, A., Natural Convection Heat Transfer in a Square Cavity Containing Nanofluid with a Vertical Plate at the Center under Magnetic Field, *Heat Transfer Research*, 45 (2014), 8, pp. 725-748
- [20] Jena, S. K., et al., Magnetoconvection of an Electrically Conducting Fluid in an Annular Space between Two Isothermal Concentric Squares, *Heat Transfer Research*, 44 (2013), 2, pp. 195-214
- [21] Nemati, H., et al., Magnetic Field Effects on Natural Convection Flow of Nanofluid in a Rectangular Cavity Using the Lattice Boltzmann Model, *Scientia Iranica*, 19 (2012), 2, pp. 303-310
- [22] Aminossadati, S. M., et al., Effects of Magnetic Field on Nanofluid Forced Convection in a Partially Heated Microchannel, *International Journal of Non-Linear Mechanics*, 46 (2011), 10, pp. 1373-1382
- [23] Patankar, S. V., Spalding, D. B., A Calculation Procedure for Heat, Mass and Momentum Transfer in Three-Dimensional Parabolic Flows, *International Journal of Heat and Mass Transfer*, 15 (1972), 10, pp. 1787-1806
- [24] Rhie, C. M., Chow, W. L., Numerical Study of the Turbulent Flow Past an Airfoil with Trailing Edge Separation, *AIAA Journal*, 21 (1983), 11, pp. 1525-1532
- [25] Ferziger, J. H., Peric, M., *Computational Methods for Fluid Dynamics*, 3<sup>rd</sup> ed., Springer Verlag, Berlin, 2002
- [26] Back, L. H., Laminar Heat Transfer in Electrically Conducting Fluids Flowing in Parallel Plate Channels, *International Journal of Heat and Mass Transfer*, 11 (1968), 11, pp. 1621-1636